Geotech Geol Eng
https://doi.org/10.1007/s10706-020-01520-1

ORIGINAL PAPER

General Analytical Solution for Laterally-Loaded Pile-Based Miche Model

Danilo C. Rosendo · Paulo J. R. Albuquerque

Received: 9 January 2020 / Accepted: 17 August 2020

Abstract Piles subjected to lateral loading can create problems in soil-structure interaction. Several differing methods of analysis have been proposed to solve the problem of laterally loaded piles, resulting in the determination of pile bending and the bending moment as a function of depth below soil surface. These piles are widely used to support laterally loaded piles, such as bridge pillars, offshore platforms, communication towers and others. This study presents an analytical solution to Miche's problem as a continuous function of depth: deflection and moment, as well as a dimensional plots to be used in projects involving piles subjected to laterally loading only including data concerning laterally loading test and pile geometry. A new formula is presented to calculate the pile head displacement as well as an equation to determine maximum moment for a generalized Miche model and further analysis. In addition, this paper proposes an equation for the determination of constant horizontal subgrade reaction (n_h) based on the CPT in-situ test and the geometric characteristics of the pile. Calibration of the analytical model showed good fit and conservative results regarding inclinometer data from an bored pile and good agreement with the literature results.

D. C. Rosendo · P. J. R. Albuquerque (✉)
University of Campinas, Campinas, Brazil
e-mail: pjra@unicamp.br

D. C. Rosendo
e-mail: daniloborralho@gmail.com

Keywords Analytical model · Laterally-loaded pile · Full-scale tests · Hypergeometric functions

1 Introduction

Piles subjected to lateral loading can create problems in soil-structure interaction. These piles are widely used to support laterally loaded structures such as bridge pillars, offshore platforms, communication towers, harbor piers, etc. Several methods, such as the constant horizontal subgrade reaction, the p–y are typically not capitalized, finite difference, finite elements, boundary and energetic elements have been proposed to solve the problem of a laterally loaded pile, whose problem can generally be defined as the determination of pile bending and the bending moment as a function of depth below the soil surface. In projects including laterally loaded piles, the determination of pile displacement plot along its depth by analytical methods, the displacement formula, as well as maximum deflection and maximum moment are challenging problems for geotechnical engineers. The fourth-order differential equation for top-loaded lateral-loading problems was first solved and numerically determined by Miche (1930), but the function that determines deflection and pile moment with depth was not clarified. It is generally possible to enumerate the commonly used mathematical methods for solving

Published online: 26 August 2020

the laterally loaded monopile problem: (i) soil reaction coefficient method: Hetenyi (1946), Miche (1930), Reese and Matlock (1960), Liang et al. (2014). (ii) curve methods: *P-Y*: Matlock (1970); Welch and Reese (1972); Reese et al. (1974), Reese and Welch (1975); Reese and Nyman (1978); API (2000), (iii) Poulos (1971a, b), Verruijt and Kooijman (1989), Zhang et al. (2000), (iv) finite element method: Banerjee and Davies (1978), Budhu and Davies (1988) and Ai et al. (2013), (v) boundary element method: Banerjee and Davies (1978), Budhu and Davies (1988) and Ai et al. (2013), (vi) variational or potential energy method: Sun (1994), Shen and Teh (2002), Basu et al. (2009), Salgado et al. (2014) and Gupta and Basu (2017). The equation numerically solved by Miche (1930) does not include the functions required to determine dislocation at any point along the depth. Froio and Rizzi (2017) present a parametric analytical form for the ordinary differential equation of an Euler–Bernoulli beam on Winkler's elastic foundation, explaining hypergeometric functions and their properties. Liang et al. (2014) obtained a simplified analytical solution for laterally loaded long piles in a soil with reaction coefficient increasing linearly according to depth by means of the Fourier–Laplace integral transform and, by using a power series, crafted a solution for small depths, through the use of asymptotic Wentzel–Kramers–Brillouin (WKB) expansion. No analytical solution was identified in the literature for this closed form of Miche's problem (1930), since the general solution is given in terms of generalized Erdélyi (1955) hypergeometric functions. Miche's model (1930) was compared with the experimental work by Albuquerque et al. (2019), who performed lateral loading testing belled caisson with the inclinometer measuring along the depth of $D = 800$ mm and length $L = 9$ m, reaching a good agreement of experimental data. In this paper, was determine the solution of the differential equation in its analytical form, as well as the displacement and moment functions to be used in designing deep foundations by piles subjected to lateral loading. The analytical solution will be compared with Miche's numerical solution (1930), literature results, displacement measurements of lateral loading tests, and inclinometer measuring. The result is the proposal of an equation used to determine displacement, the moment along the depth and at the top, the equations used to determine the maximum moments for various variation laws of the constant horizontal subgrade reaction, and a fractional model to solve the problem. This study will be calibrated by means of an analytical equation with use of a laterally loading test, with inclinometer measurements along the pile length, which are bored pile type with $D = 300$ mm and length $L = 5$ m, in the Experimental Site of Foundations University of Campinas, São Paulo State, Brazil.

2 The Miche Model

Miche (1930) was one of the first to solve the problem of the laterally loaded pile at the top, with the constant horizontal subgrade reaction increasing linearly with depth, assuming the Winkler hypothesis and considering the free top with the load applied to the surface (Fig. 1). The differential equation for the Miche model is provided as:

$$E_p I_p \frac{d^4 y}{dz^4} + n_h z y = 0, \tag{1}$$

where E_p = pile elasticity modulus, Ip = pile moment of inertia, n_h = proportional constant for horizontal subgrade reaction with depth, y = pile lateral deflection with respect to vertical axis z.

For the solution of Eq. (1) the relative stiffness factor T was defined by, Van Impe and Reese (2010) of pile for this problem, as:

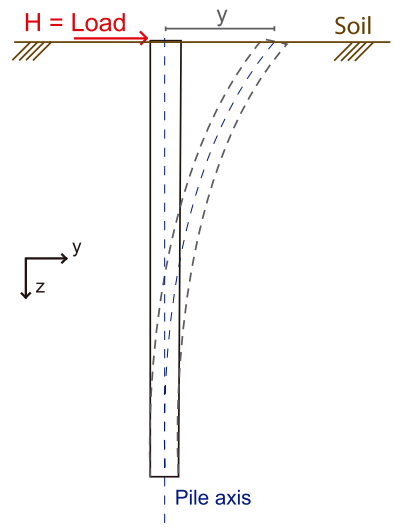

Fig. 1 Laterally loaded top pile

$$T = \sqrt[5]{\frac{E_p I_p}{n_h}}. \tag{2}$$

And for practical design issues, β is defined as the inverse of the relative stiffness factor of pile, ie $\beta = \frac{1}{T}$.

The analytical solution of differential Eq. (1) is made by a power series in terms of the Erdélyi (1955) generalized hypergeometric functions, which are defined as follows:

$${}_pF_q(a_1, a_2, \ldots, a_q; b_1, b_2, \ldots, b_p; z) = \sum_{n=1}^{\infty} \frac{\prod_{j=1}^{p} (a_j)_n}{\prod_{j=1}^{q} (b_j)_n} \frac{z^n}{n!} \tag{3}$$

where in the a_j numbers are called parameters the numerator p, the b_j numbers are referred to as parameters of denominator q and $(a)_n$ indicates the Pochhammer symbol, defined as:

$$(a_j)_n = a_j(a_j + 1) \cdots (a_j + n - 1) = \frac{\Gamma(a_j + n)}{\Gamma(a_j)} \tag{4}$$

and $\Gamma(z)$ is the gamma function.

Equation (1) is a homogeneous linear ordinary differential equation, and its solution is made with a linear combination of four linearly-independent functions King et al. (2003). The general solution of Eq. (1) is provided in:

$$y(z) = a_0 y_1(z) + a_1 y_2(z) + a_2 y_3(z) + a_3 y_4(z) \tag{5}$$

where a_0, a_1, a_2 and a_3 are constants to be determined according to the boundary conditions of the problem, and y_i with $i = 1, 2, 3, 4$ are linearly independent solutions Oliveira and Tygel (2005). The analytical solution of this equation is provided by the high order equation power series method proposed by Robin (2014), knowing that $z_0 = 0$ is an ordinary point Eq. (1), its solution in the following form:

$$y(z) = \sum_{n=0}^{\infty} a_n z^n \tag{6}$$

where a_n are the coefficients of the power series to be determined. This Taylor series solution can be rewritten in the form of generalized hypergeometric functions, that is, as follows:

$$\begin{aligned} y[z] = {} & a_0 \, {}_0F_3\left(;\frac{2}{5},\frac{3}{5},\frac{4}{5};-\frac{1}{625}z^5\beta^5\right) \\ & + a_1 z 5^{-4/5} \beta \, {}_0F_3\left(;\frac{3}{5},\frac{4}{5},\frac{6}{5};-\frac{1}{625}z^5\beta^5\right) \\ & + a_2 z^2 5^{-8/5} \beta^2 \, {}_0F_3\left(;\frac{4}{5},\frac{6}{5},\frac{7}{5};-\frac{1}{625}z^5\beta^5\right) \\ & + a_3 z^3 5^{-12/5} \beta^3 \, {}_0F_3\left(;\frac{6}{5},\frac{7}{5},\frac{8}{5};-\frac{1}{625}z^5\beta^5\right) \end{aligned} \tag{7}$$

where a_0, a_1, a_2 and a_3 are the constants to be determined in accordance with the pile boundary conditions, and β is inverse relative stiffness factor. This is Miche's analytical formula. For situation $\beta = 1$, the generalized hypergeometric functions are represented in Fig. 2.

In order to determine the analytical solution of the Miche (1930) problem, the following boundary conditions apply:

1. At the top of the pile:

$$y'''[0] = \frac{H}{E_p I_p}; y''[0] = 0 \tag{8}$$

2. At the base of the pile:

   (a) condition 01;

$$y'[L] = 0; \quad y[L] = 0 \tag{9}$$

   (b) condition 02;

$$y''[L] = 0; \quad y'''[0] = 0 \tag{10}$$

The main problem with lateral loading is the determination of the displacement and moment functions along the depth of the pile when top loading is applied. Thus, the determination of displacement at the load application site, the maximum moments and where it is located in relation to the soil surface can be made explicit. Given the lateral loading H at the top of the pile ($z = 0$) and the boundary conditions are provided by Eqs. (8) and (9); the analytical solution of the displacement function along the pile depth, the moment function along depth, and its maximum points can be determined. Taking into account the general analytical solution of Miche (1930) problem is provided by Eq. (7), with the boundary conditions provided in Eqs. (8) and (10), by replacing these

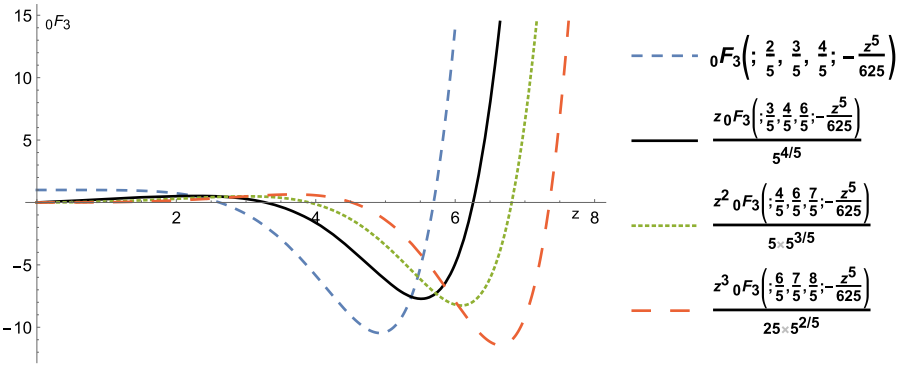

Fig. 2 Generalized hypergeometric functions, $\beta = 1$

conditions and solving the system of equations, the values for a_0, a_1, a_2 and a_3 are acquired with use of Eqs. (11)–(14).

$$a_o = \frac{-H}{E_P I_p} \cdot \frac{\left(-2016L^3A \cdot B - 14L^8\beta^5 B \cdot F + 3L^8\beta^5 D \cdot A\right)}{84\left(72A \cdot E + 3L^5\beta^5 A \cdot C - L^5\beta^5 E \cdot F\right)} \tag{11}$$

$$a_1 = \frac{-H}{E_P I_p} \cdot \frac{\left(1008L^2E \cdot B + 14L^7\beta^5 B \cdot C - L^7\beta^5 D \cdot E\right)}{28\beta\left(72A \cdot E + 3L^5\beta^5 A \cdot C - L^5\beta^5 E \cdot F\right)} \tag{12}$$

$$a_2 = 0 \tag{13}$$

$$a_3 = \frac{H}{6\beta^3 E_P I_p} \tag{14}$$

The functions A, B, C, D, E and F, are provided by the Eq. (15):

$$\begin{aligned}
A[L,\beta] &= {}_0F_3\left(;\frac{3}{5},\frac{4}{5},\frac{6}{5};-\frac{1}{625}\beta^5L^5\right),\\
B[L,\beta] &= {}_0F_3\left(;\frac{6}{5},\frac{7}{5},\frac{8}{5};-\frac{1}{625}\beta^5L^5\right),\\
C[L,\beta] &= {}_0F_3\left(;\frac{7}{5},\frac{8}{5},\frac{9}{5};-\frac{1}{625}\beta^5L^5\right),\\
D[L,\beta] &= _0F_3\left(;\frac{11}{5},\frac{12}{5},\frac{13}{5};-\frac{1}{625}\beta^5L^5\right),\\
E[L,\beta] &= {}_0F_3\left(;\frac{2}{5},\frac{3}{5},\frac{4}{5};-\frac{1}{625}\beta^5L^5\right),\\
F[L,\beta] &= {}_0F_3\left(;\frac{8}{5},\frac{9}{5},\frac{11}{5};-\frac{1}{625}\beta^5L^5\right),
\end{aligned} \tag{15}$$

The exact analytical displacement function solution to the Miche (1930) problem is provided by Eq. (16):

$$\begin{aligned}
y[z] = {} & \frac{-H}{E_P I_p}\frac{\left(-2016L^3A \cdot B - 14L^8\beta^5 B \cdot F + 3L^8\beta^5 D \cdot A\right)}{84\left(72A \cdot E + 3L^5\beta^5 A \cdot C - L^5\beta^5 E \cdot F\right)}\\
& {}_0F_3\left(;\frac{2}{5},\frac{3}{5},\frac{4}{5};-\frac{1}{625}z^5\beta^5\right)\\
& + z5^{-4/5}\beta\frac{-H}{E_P I_p}\frac{\left(1008L^2E \cdot B + 14L^7\beta^5 B \cdot C - L^7\beta^5 D \cdot E\right)}{28\beta\left(72A \cdot E + 3L^5\beta^5 A \cdot C - L^5\beta^5 E \cdot F\right)}\\
& {}_0F_3\left(;\frac{3}{5},\frac{4}{5},\frac{6}{5};-\frac{1}{625}z^5\beta^5\right)\\
& + z^3 5^{-12/5}\beta^3\frac{H}{6\beta^3 E_P I_p}{}_0F_3\left(;\frac{6}{5},\frac{7}{5},\frac{8}{5};-\frac{1}{625}z^5\beta^5\right)
\end{aligned} \tag{16}$$

The top displacement of the pile when the load is applied at this point $(z = 0)$ is provided by Eq. (13), Miche (1930):

$$y[0] = 2.4\frac{HT^3}{E_pI_p}. \tag{17}$$

Equation (17) does not depend on pile length along the depth, but for the exact analytical model, we have the influence of pile length on top displacement, since if $z = 0$ in Eq. (16), then:

$$y[0] = \frac{-H}{E_PI_p}\cdot\frac{\left(-2016L^3A\cdot B - 14L^8\beta^5B\cdot F + 3L^8\beta^5D\cdot A\right)}{84\left(72A\cdot E + 3L^5\beta^5A\cdot C - L^5\beta^5E\cdot F\right)} \tag{18}$$

where functions A, B, C, D, E and F are provided by Eq. (15). The moment function is calculated by the second derivative of the displacement function in Eq. (19).

$$M[z] = E_pI_p\frac{d^2y}{dz^2} \tag{19}$$

Followed by the moment function in (20):

$$\begin{aligned} M[z] = {} & z\,{}_0F_3\left(;\frac{6}{5},\frac{7}{5},\frac{8}{5};-\frac{1}{625}z^5\beta^5\right) \\ & + \frac{\beta^{10}z^{11}\,{}_0F_3\left(;\frac{16}{5},\frac{17}{5},\frac{18}{5};-\frac{1}{625}z^5\beta^5\right)}{3459456} \\ & - \frac{1}{6}a_0\beta^5z^3\,{}_0F_3\left(;\frac{7}{5},\frac{8}{5},\frac{9}{5};-\frac{1}{625}z^5\beta^5\right) \\ & + \frac{a_0\beta^{10}z^8\,{}_0F_3\left(;\frac{12}{5},\frac{13}{5},\frac{14}{5};-\frac{1}{625}z^5\beta^5\right)}{12096} \\ & - \frac{1}{12}a_1\beta^6z^4\,{}_0F_3\left(;\frac{8}{5},\frac{9}{5},\frac{11}{5};-\frac{1}{625}z^5\beta^5\right) \\ & + \frac{a_1\beta^{11}z^9\,{}_0F_3\left(;\frac{13}{5},\frac{14}{5},\frac{16}{5};-\frac{1}{625}z^5\beta^5\right)}{57024} \\ & - \frac{5\beta^5z^6\,{}_0F_3\left(;\frac{11}{5},\frac{12}{5},\frac{13}{5};-\frac{1}{625}z^5\beta^5\right)}{1008}, \end{aligned} \tag{20}$$

where a_0 and a_1 are functions provided by Eqs. (11) and (12). The shear force function is calculated by the third derivative of the displacement function, or as Eq. (21):

$$Q[z] = E_pI_p\frac{d^3y}{dz^3} \tag{21}$$

2.1 The Proposed Generalized Miche Model

The generalized Miche model is provided by Eq. (22):

$$E_pI_p\frac{d^4y}{dz^4} + n_hz^\lambda y = 0 \tag{22}$$

where E_p = pile Young modulus, I_p = pile moment of inertia, n_h = proportional constant for the horizontal soil reaction coefficient, E = soil Young modulus and positive rational λ. The solution of Eq. (22) for $\lambda > 1$ follows a similar power series resolution procedure applied to obtain the analytical solution when $\lambda = 1$. Miche's generalized equation corresponds to the power function as by Matlock and Reese (1961a) as $K_h = kz^n$. The general solution of Eq. (22) for an exponent $\lambda = n$ is provided by Eq. (23):

$$\begin{aligned} y[z] = {} & c_1\,{}_0F_3\left(;1-\frac{3}{n+4},1-\frac{2}{n+4},1-\frac{1}{n+4};-\frac{z^{n+4}\beta^5}{(n+4)^4}\right) \\ & + c_2(n+4)^{-\frac{4}{n+4}}z\beta^{\frac{5}{n+4}}\,{}_0F_3 \\ & \left(;1-\frac{2}{n+4},1-\frac{1}{n+4},1+\frac{1}{n+4};-\frac{z^{n+4}\beta^5}{(n+4)^4}\right) \\ & + c_3(n+4)^{-\frac{8}{n+4}}z^2\beta^{\frac{10}{n+4}}\,{}_0F_3 \\ & \left(;1-\frac{1}{n+4},1+\frac{1}{n+4},1+\frac{2}{n+4};-\frac{z^{n+4}\beta^5}{(n+4)^4}\right) \\ & + c_4(n+4)^{-\frac{12}{n+4}}z^3\beta^{\frac{15}{n+4}}\,{}_0F_3 \\ & \left(;1+\frac{1}{n+4},1+\frac{2}{n+4},+1+\frac{3}{n+4};-\frac{z^{n+4}\beta^5}{(n+4)^4}\right) \end{aligned} \tag{23}$$

where c_1, c_2, c_3 and c_4 are constants to be determined according to pile boundary conditions.

2.2 The Miche Fractional Model

The fractional Miche model is more generalized than Eq. (1), since the term of the fourth derivative will be replaced by any real and positive exponent. The equation has the following form:

$$E_pI_p\frac{d^\alpha y}{dz^\alpha} + n_hz^ny = 0, \tag{24}$$

where $3 < \alpha \leq 4$ and n the exponent of the proportional constant horizontal soil reaction coefficient.

3 Experimental Tests

Experimental field trials were performed to calibrated the results, and they were performed in order to clarify the behavior of single piles subjected to horizontal top

loading through horizontal loading tests. Laboratory and in situ tests were performed in the experimental Site at Unicamp, for geotechnical characterization, with the objective of calibration the analytical models developed in this study.

3.1 Experimental Field Geology

The geological–geotechnical profile and the average parameters for each soil layer were previously obtained through laboratory tests performed by Gon (2011). The average soil profile parameters for the layers were obtained by average tests of seven SPT and three CPT, reaching impenetrable percussion, which is summarized in the Table 1.

According to Gon (2011), an average soil profile was developed for the Experimental site subsoil where the averages of each parameter, standard deviation and coefficient of variation were determined. The best result among the values of the coefficient of variability between parameters was used to define the layers. Garcia (2015) defines an average soil profile, provided in the table shown in Table 1.

3.2 Lateral Load Test

Preparation of the tests followed the standard recommendations of *D*3966 (ASTM 2013), which provides a test method for deep foundations under lateral loads. Test loadings were carried out on bored piles of $D = 300$ mm and length $L = 5$ m, and an 80 mm aluminum tube was placed inside the pile to read the inclinometer. These piles were made with use of a helical auger connected to a metal rod attached to a truck. The piles was fully reinforced along their length, where 6 longitudinal 10 mm diameter CA-50 steel bars and 5 mm diameter CA-50 steel stirrups were placed every 15 cm. The lateral loading test on the pile followed the scheme shown in Fig. 3, where the reaction was caused by a three-pile block, the hydraulic jack for load application, the displacement transducers (LVDT) and the inclinometers to measure displacement along depth.

Maximum load occurred at 49 kN with a displacement of 14.10 mm, the graph in Fig. 4 shows the curve load versus load test displacement. In the laterally loaded piles design, the performance of the lateral loading test is defined as a ultimate load. However, for the design of a pile under lateral loading and deflection prediction along the depth, it was used the allowable load which is the ultimate load divided by the safety factor. From the results of the load test, it was possible to obtain the load versus displacement curve (Fig. 5).

The readings with the inclinometer allowed to obtain the variation of the horizontal displacements in depth. The results obtained are presented as a graph in Fig. 5 indicating the incremental and cumulative variation of the displacements in relation to the pile depth, for each load stage in the horizontal loading test.

3.3 Modulus of Subgrade Reaction Soil

The concept of the modulus of horizontal reaction of the soil (K) defined as the relationship between the soil reaction (in units of force applied along the pile

Table 1 Soil classification by SPT and CPT test

Depth (m)	Nspt	q_c (MPa)	f_s (MPa)	Rf (%)	Robertson (1990)	Vos (1982)	SUCS
1	2	2.4	0.119	4.9	Silty clay and clayey silt	Clay	MH
2	4	1.4	0.035	2.5	Silty sand and silt	Silt	ML
3	4	1.4	0.038	2.8	Silty sand and silt	Silt	ML
4	5	1.8	0.050	2.8	Silty sand and silt	Silt	ML
5	6	2.3	0.064	2.8	Silty sand and silt	Silt	ML
6	6	2.5	0.077	3.1	Silty sand and silt	Clay	ML
7	7	3.2	0.090	2.9	Silty sand and silt	Silt	ML
8	8	3.0	0.104	3.5	Silty sand and silt	Clay	ML
9	24	2.1	0.126	6.0	Clay	Clay	MH
10	36	5.8	0.173	3.0	Silty sand and silt	Silt	MH

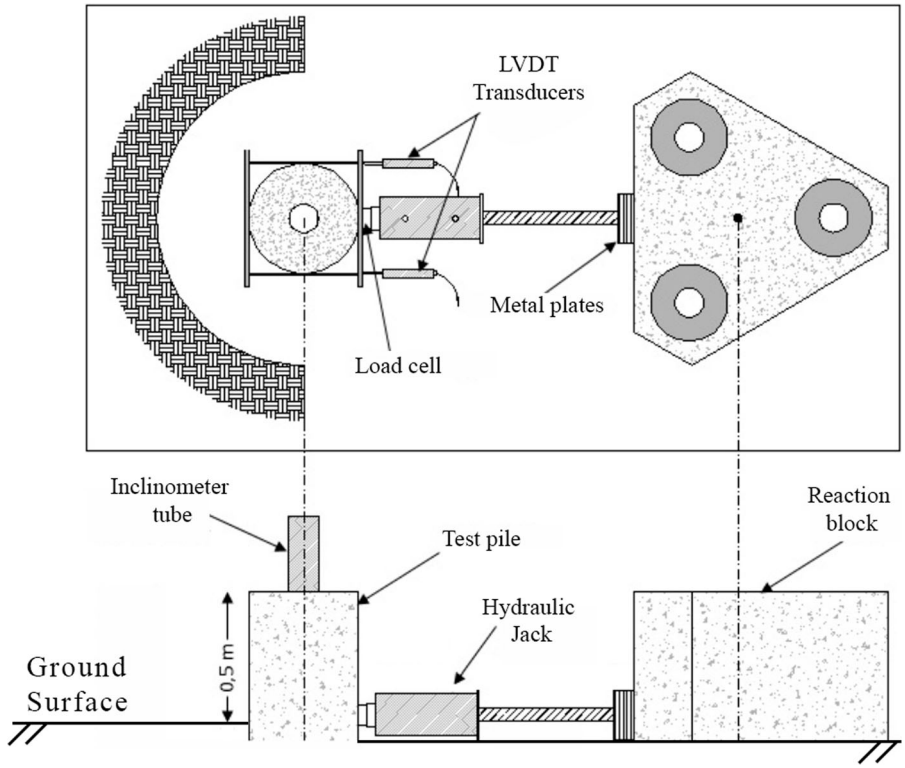

Fig. 3 Lateral loading test scheme

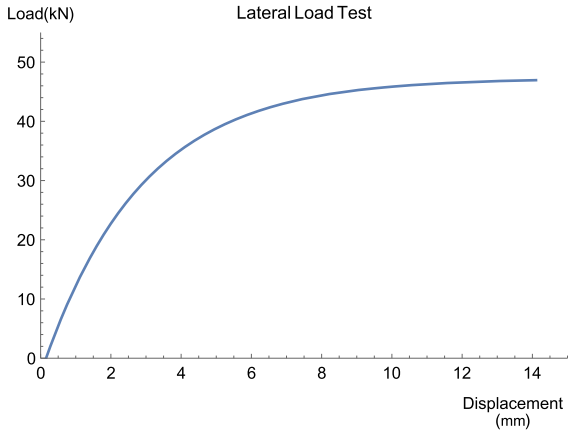

Fig. 4 Result the lateral loading test

length) and the corresponding displacement, Van Impe and Reese (2010), with Eq. (25):

$$K = \frac{P}{y} \tag{25}$$

where K = modulus of horizontal reaction (FL^{-2}); p = applied force (FL^{-1}); and y = horizontal displacement (L).

For pure sand, the Young's modulus increases (approximately) linearly with depth. Therefore, the soil reaction to the load applied to the pile is assumed to increase linearly with depth

$$K = n_h z \tag{26}$$

where n_h = constant horizontal reaction subgrade soil (FL^{-3}); and z = depth (L).

The modulus horizontal reaction is not a soil parameter, but that it depends on soil resistance and pile deflection (Van Impe and Reese 2010).

According to Van Impe and Reese (2010) for a given soil profile, the soil-reaction modulus is influenced intrinsically by the following variables: pile type and flexural stiffness, short or long term, type loading, pile geometry, pile installation procedure.

Several researchers have studied the behavior of the coefficient of horizontal reaction such as: Biot, Terzaghi, Veisic, Vlassov, Bowles, Selvadurai and

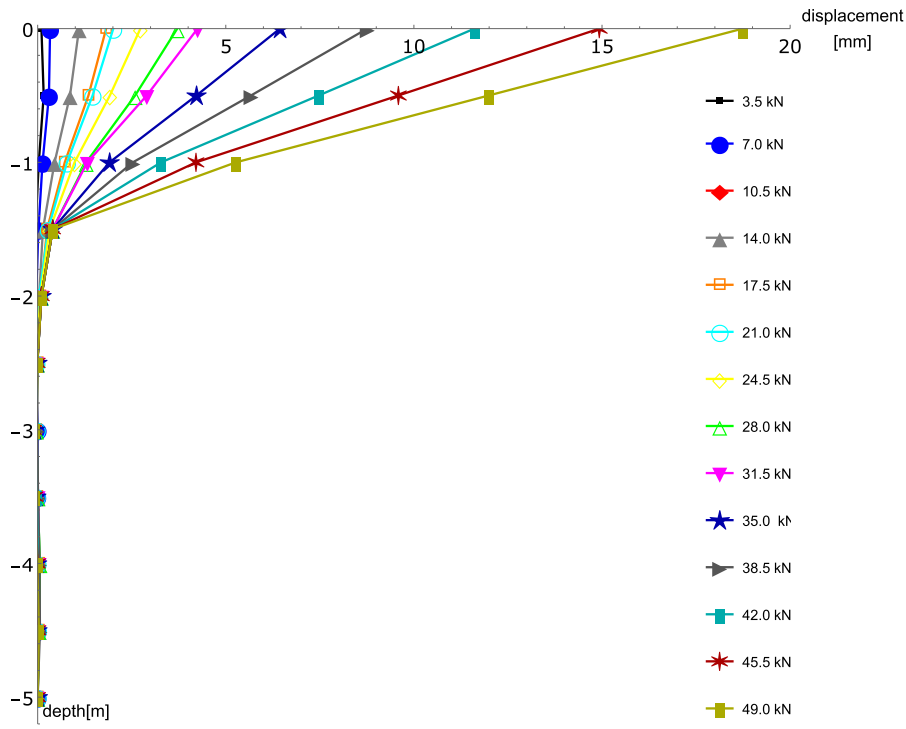

Fig. 5 Inclinometer reading according to depth

others, but most formulas are based on soil and pile elasticity module, Possion coefficient, stiffness at flexion but few models take into account the horizontal load and deflection of the pile. Equations that depend on the load, and some geotechnical parameters are found in the work Phanikanth et al. (2013), in this paper presented an equation in this way that will have an experimental adjustment with in-situ data in relation to the average values in the case of the sands as a function of the specific weight and angle of friction and for clay soils of specific weight and cohesion, but depending on the load or maximum displacement at the top of the pile.

According to Matlock and Reese (1961a), it is not possible to determine a single value for the constant horizontal subgrade reaction (n_h) because the lateral load test is a load versus non-linear displacement curve. In the paper of Matlock and Reese (1961a), for isolated piles, an interval is determined for y_0, from 6 to 12 mm, to find the n_h the arithmetic average is calculated. Alizadeh and Davisson (1970) were the first to present the results of showing a graph of the variation of the horizontal reaction coefficient on the y axis and y_0 displacement, of lateral load tests on sandy soil and used a variation of 6.35–12.7 mm to determine n_h. Matlock (1970) used a range of 6–12 mm for the determination of n_h. All of these studies relate the constant horizontal subgrade reaction of the soil to the data of the lateral loading test for the pile in a given soil, thus having the horizontal reaction coefficient of the soil pile set with the displacement and load limit, which in most tests of side load the displacement at the top is less than 5% D, where D is the diameter.

The constant horizontal subgrade reaction of the isolated pile can be determined mathematically, according to Matlock and Reese (1961a) with the variations of y_0 between 4 and 8 mm is determined numerically, replacing these values, respectively, in the Eq. 27, where $n_h(4) = 29.29\,\mathrm{MN/m^3}$ and $n_h(8) = 15.98\,\mathrm{MN/m^3}$, making the arithmetic average result $n_h = 22.64\,\mathrm{MN/m^3}$. The horizontal reaction coefficient of the soil of the isolated pile, with the variations of y_0 between 6 and 12 mm is 13.72 MN/m^3.

The constant horizontal subgrade reaction of the soil (n_h) for the isolated pile varies with the values of the displacement y_0, according to the data of the inclinometer, given by Fig. 6, was adjusted by the

method of least squares, in the graph of Fig. 6, it has the following expression:

$$n_h(y_0) = 161.15e^{-0.95y_0} - 2.45y_0 + 35.52 \quad (27)$$

An equation to calculate the horizontal reaction coefficient of the soil n_h was adjusted, according to the equation of Phanikanth et al. (2010), and using the method of least squares, for average data of the experimental test, such that:

$$n_h = \frac{560C_\phi \gamma^{1.5}\sqrt{E_pI_pD}}{H} \quad (28)$$

where $C_\phi = 3 \cdot 10^{-5}(1,316)^{\phi}$, ϕ—friction angle, γ - specific weight, H - load, E_pI_p—pile flexural stiffness and D—diameter pile.

According data Table 2 the average value of the specific gravity of the soil is approximately $14.5\,\mathrm{kN/m^3}$ and the friction angle is 22.4°, so the value of the constant horizontal subgrade reaction soil for a load 49 kN is replacing in the Eq. 28, $n_h = 13.52\,\mathrm{kN/m^3}$. A graph to represent the Eq. (28) is given in Fig. 7.

A new equation for the constant horizontal subgrade reaction is presented with the CPT in-situ test data, through a least squares adjustment of the parameters of the cone resistance q_c and the sleeve friction resistance f_s in relation to the friction angle (ϕ) and specific weight (γ), according to Robertson and Cabal (2015).

$$\phi(^\circ) = 21.16 + \log\frac{q_c^{1.4}}{f_s^{1.76}} \quad (29)$$

$$\gamma(\mathrm{kN/m^3}) = 23.71 + \log\frac{f_s^{0.55}}{q_c^{0.45}} \quad (30)$$

Replacing the Eqs. (29) and (30) in the Eq. (28), and using the expansion of powers, result

$$n_h(\mathrm{kN/m^3}) = \frac{0.43q_c^{0.38}e^{\frac{6.53q_c^{0.025}}{f_s^{0.02}}}\sqrt{E_pI_pD}}{f_s^{0.18}H} \quad (31)$$

where H—load and E_pI_p—pile flexural stiffness.

The Eq. (31) is the relationship between the soil parameters and the horizontal soil reaction constant for the experimental site data, for a general expression was done a retro-analysis of the load tests and have the geotechnical parameters of the laboratory tests and the CPT in-situ tests.

4 Results

The analytical solutions obtained in this paper will first be compared with Miche's method (1930) for displacement, moment and shear. It will also analyze the relation of top displacement as a function of depth and characteristic stiffness. Afterwards, the generalized Miche model proposed for $K_h = kz^n$, where $n = 1, 2, 3, 4, 5, 6, 7$ and 8, is compared to the functions of displacement and moment, and an equation to

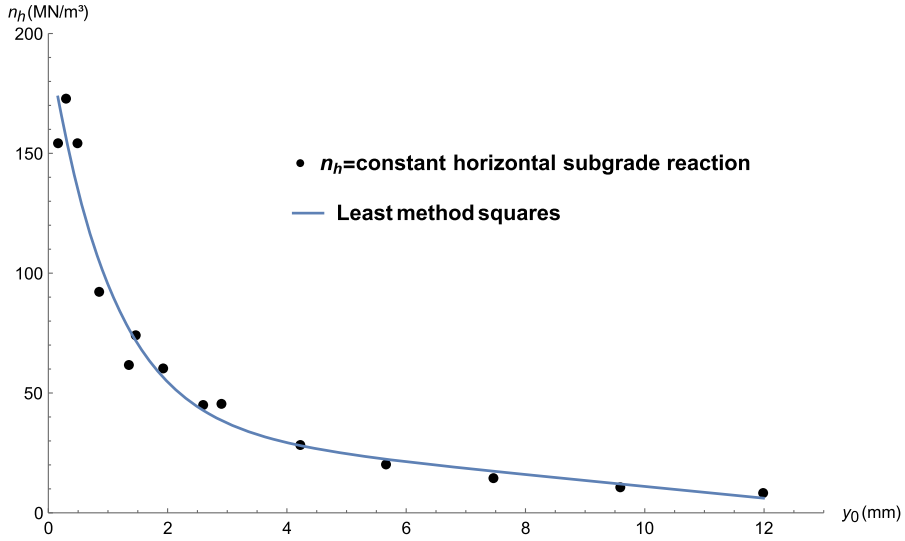

Fig. 6 Constant horizontal reaction subgrade soil of the single pile with fit least square

Table 2 General properties at Unicamp experimental site, Gon (2011)

Deph (m)	N_{spt}	SUCS	γ_s (kN/m^3)	w (%)	Suction (kPa)	c' (kPa)	ϕ'	E_s (MPa)	k_0
1	2.0	MH	14.1	28.3	43.0	7.4	22°	13.8	0.6
2	3.9	ML	14.2	27.9	55.0	7.9	21°	11.4	0.6
3	4.0	ML	14.0	28.0	39.0	11.6	22°	8.5	0.6
4	5.3	ML	14.4	25.5	85.0	5.8	23°	11.5	0.6
5	6.0	ML	15.5	26.2	–	24.0	21°	9.9	0.6
6	6.3	ML	15.3	26.1	110.0	42.4	22°	20.0	0.6
7	6.9	ML	15.4	28.3	20.0	41.9	22°	10.9	0.6
8	7.9	ML	15.2	32.3	–	26.4	22°	11.0	0.6
9	23.6	MH	15.2	40.6	–	–		–	–

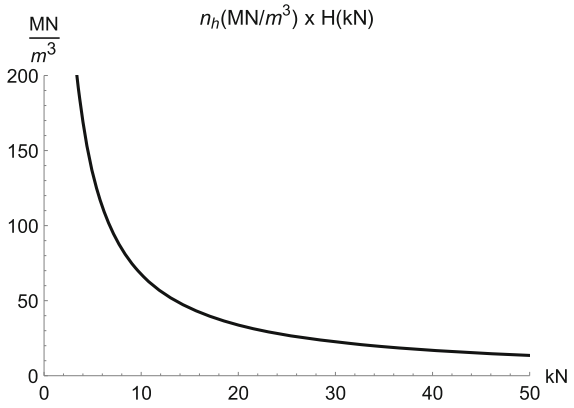

Fig. 7 Constant horizontal reaction subgrade n_h versus load H

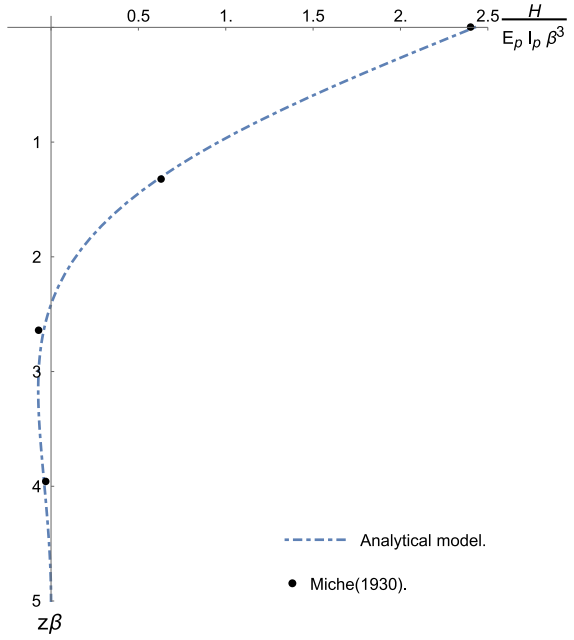

Fig. 8 Analytical displacement function

calculate the maximum moment is proposed. The analytical solution is compared with the literature results, and lastly the model is calibrated with measurement data from the inclinometer of an bored pile and pipe.

4.1 Miche Analytical Solution and Model

Miche's (1930) solution does not present the method used to solve Eq. (1), nor does it explain the displacement function along depth. With the continuous and exact displacement function, displacements can be determined at any point along the pile, thus leading to better calibration with the inclinometer data along the length. Figure 8 shows the displacements expressed in Eq. (16), which is then compared to the results of Miche (1930) in the graph of Fig. 8.

The exact analytical moment function is shown in Eq. (20) and represented in the graph of Fig. 9 in comparison with Miche's model (1930). The analytical model has a good numerical agreement for values smaller than $z \leq 4\beta$, because Miche's model (1930) includes an error related to the analytical model.

The shear function is represented in the graph of Fig. 10 comparing the analytical shear function with Miche's model (1930), an error in the points above $z \leq 2.5$ can be seen.

For different depths it is possible to observe a variation of displacement depending on relative stiffness (β), but when the pile length is greater than 9 m, it no longer influences top displacement, this can be seen in the graph of Fig. 11.

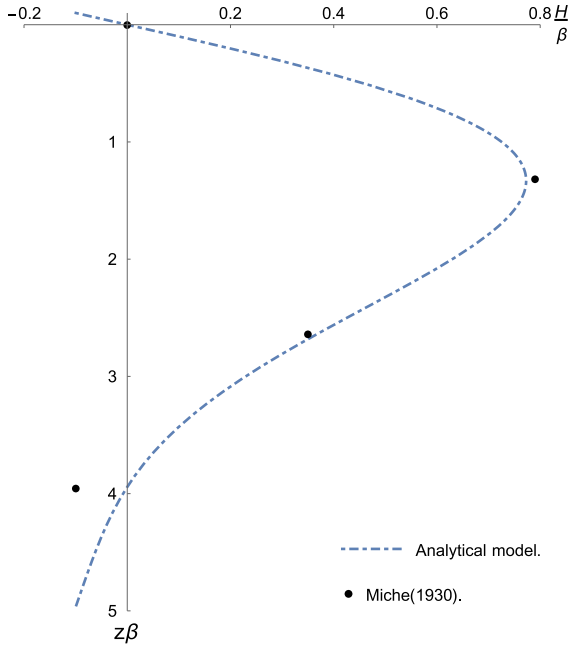

Fig. 9 Exact analytical moment function

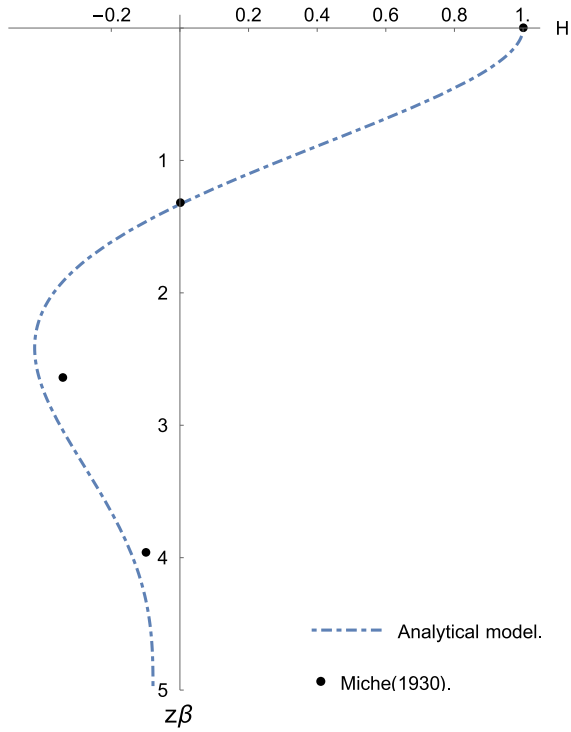

Fig. 10 Exact analytical shear function and Miche (1930)

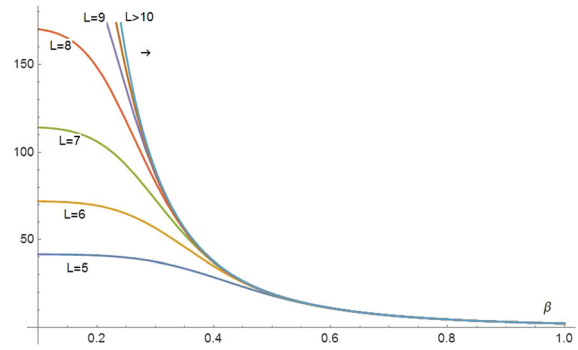

Fig. 11 Top displacement with $(z = 0)$ with stiffness variation (β)

4.2 Comparison with Literature Results

Liang et al. (2014) obtained a simplified analytical solution by means of an integral Fourier–Laplace transform for long laterally loaded piles on a soil with reaction coefficient increasing linearly with depth, but the model shows one discontinuity, in that the analytical model function is continuous across the length of the pile, the graph shown in Fig. 12 compares the solutions.

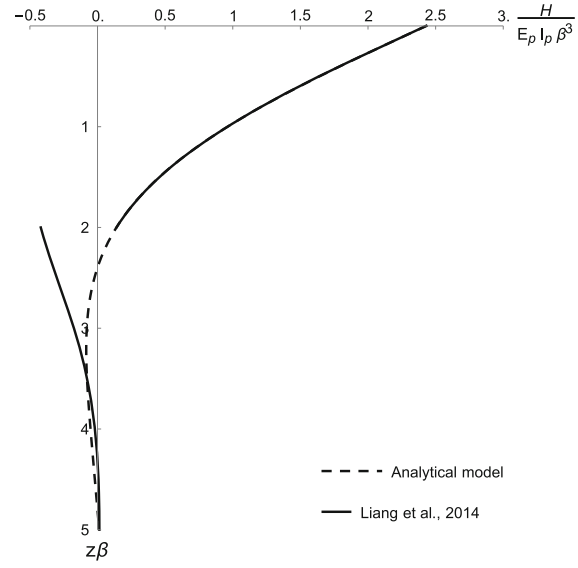

Fig. 12 Comparison between analytical model and Liang et al. (2014)

4.2.1 Generalized Miche Model

As for the generalized Miche model, the variation of the displacement and moment functions with values up to $n = 8$ will be analyzed. The displacement functions increase from $n = 1$ to $n = 4$, and then decrease to values from $n = 5$ to $n = 8$, and even with different values displacements have similar values, as can be seen in the graphs of Figs. 13 and 14.

The moment functions raise when n grows, from $n = 1$ to $n = 4$, Fig. 15. The application point, starting from the maximum moment, increases the values $n = 1$ to $n = 4$, and after $n = 6$ to $n = 8$, it presents similar values (Fig. 16). The maximum values of the moment functions of $n = 1$, $n = 2$, $n = 3$, $n = 4$, $n = 5$, $n = 6$, $n = 7$ and $n = 8$ were determined numerically, as well as their application point in Table 3. It was divided into two sections for adjustment, and so it has two functions for maximum moment. Afterwards, a non-linear fit by the least squares method Ayyub and McCuen (2015) for $n = 1$ to $n = 5$, where it has the following fit equation showing in 32.

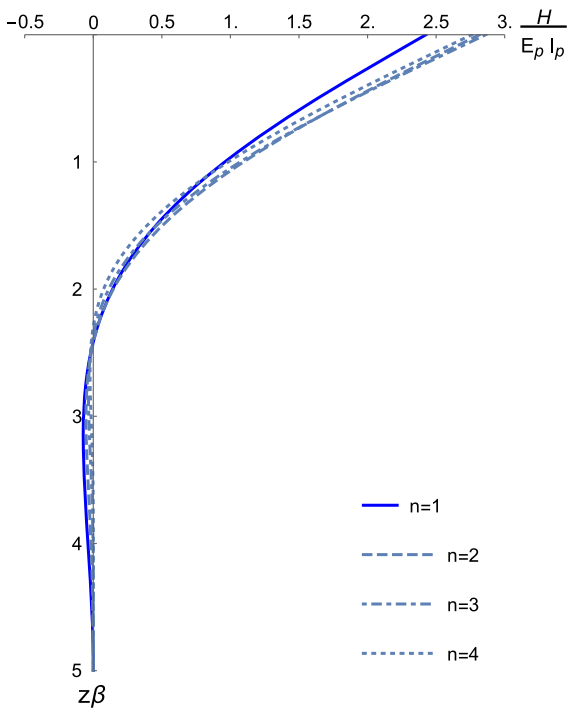

Fig. 13 Comparison of Miche's analytical displacement functions, with $n = 1$, $n = 2$, $n = 3$ and $n = 4$

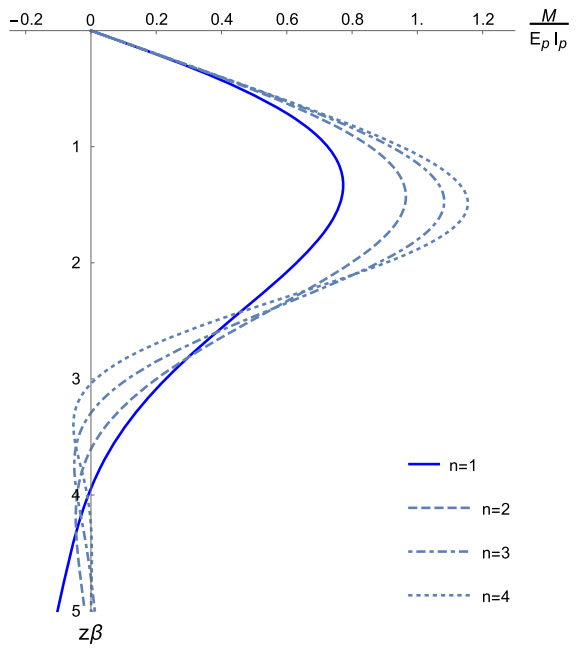

Fig. 14 Comparison of Miche's analytical displacement functions, with $n = 1$, $n = 5$, $n = 6$, $n = 7$ and $n = 8$

Table 3 Maximum moments and application points for each value of n

n	$\frac{z}{\beta}$	$\frac{M_{max}}{H/\beta}$
1	1.3308	0.7727
2	1.4287	0.9648
3	1.4718	1.0822
4	1.4864	1.1546
5	1.4863	1.1998
6	1.478	1.2279
7	1.467	1.2453
8	1.453	1.2554

$$M_{\max} = \frac{H}{\beta} 0.269 \ln (17.89n) \tag{32}$$

where n is the power of the generalized Miche model so that $0 < n < 6$; $M_{\max}$ is maximum moment, H is top loading and β is the inverse of the ground pile's relative stiffness. The maximum moment of the moment functions for values from $n = 6$ to $n = 8$ is

$$M_{\max} = \frac{H}{\beta} (0.9702 + 0.06485n - 0.00365n^2) \tag{33}$$

where n is the power of the generalized Miche model such that $5 < n < 9$; $M_{\max}$ is the maximum moment, H is top loading and β is the inverse of the ground pile

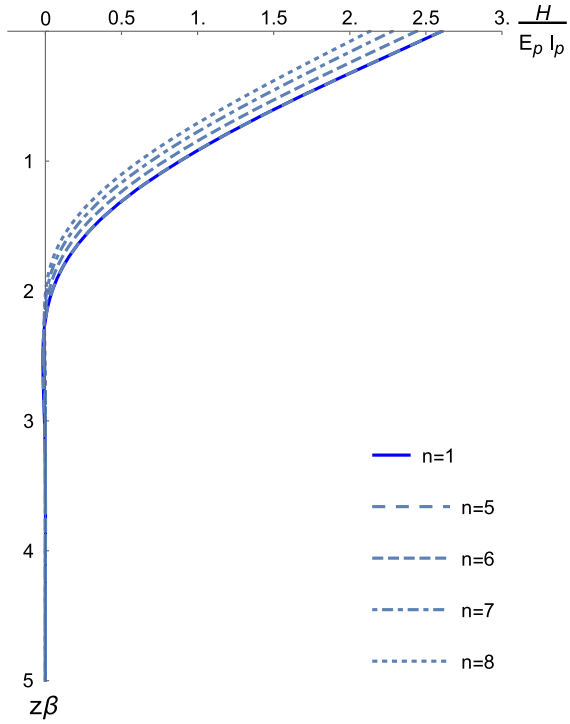

Fig. 15 Comparison of Miche's analytical moment function, with $n = 1$, $n = 2$, $n = 3$ and $n = 4$

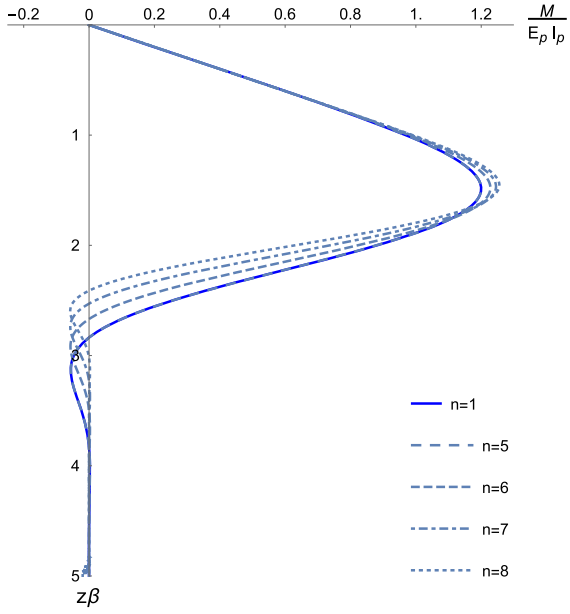

Fig. 16 Comparison of Miche's analytical moment functions, with $n = 1$, $n = 5$, $n = 6$ $n = 7$ and $n = 8$

relative stiffness. The application points and the maximum moments were determined by numerical search of the extreme points of the moment functions, summarized in Table 3.

4.3 Constant Horizontal Subgrade Reaction

Comparing the result of the constant horizontal subgrade reaction of the soil, in the graph of Fig. 17, obtained from the lateral loading test with the Eq. (31), it is noted that the curves have approximate results in the displacement range between 6 and 12 mm.

The difference in inflection in the graphs, in Fig. 17, slightly changes the results of n_h, since the authors' Matlock and Reese (1961b) are for values than 4 mm, in the Table 4. The values of the constant horizontal subgrade reaction soil were numerically determined.

The constant horizontal subgrade reaction of the soil is determined by the methodology of Matlock and Reese (1961b) and Alizadeh and Davisson (1970) with that is determined through the Eq. (31), had close values thus showing the good agreement of the results of the lateral load test and the CPT in situ test.

4.4 Model Calibration

For calibration of the analytical model, was used data from the inclinometer in a bored pile. During data analysis, it was considered the displacement of each foundation on the $y = Y$ axis and the depth on the $z = Z$ axis according to the shape of Fig. 18.

Albuquerque et al. (2019) conducted a lateral loading test on a belled caisson, 80 cm in diameter and 9 m in length with inclinometer measuring along depth a load of $H = 180$ kN. Miche's analytical model from Eq. (1), with the following conditions $E_pI_py'''(z) = H$, $E_pI_py''(z) = 0$, $y''(0) = 0$, $y''(9) = 0$ and $y'''(9) = 0$, gives the exact solution of the displacement equation as a function of depth in the graph shown in Fig. 19. The analytical model for $n = 1$ had good agreement with the experimental results. Since the ultimate load for the pile was 180 kN, this analytical model does not behave well with values close to the ultimate, since the plasticization of the soil and concrete are not taken into account. However, for design values one can predict the behavior of the deep

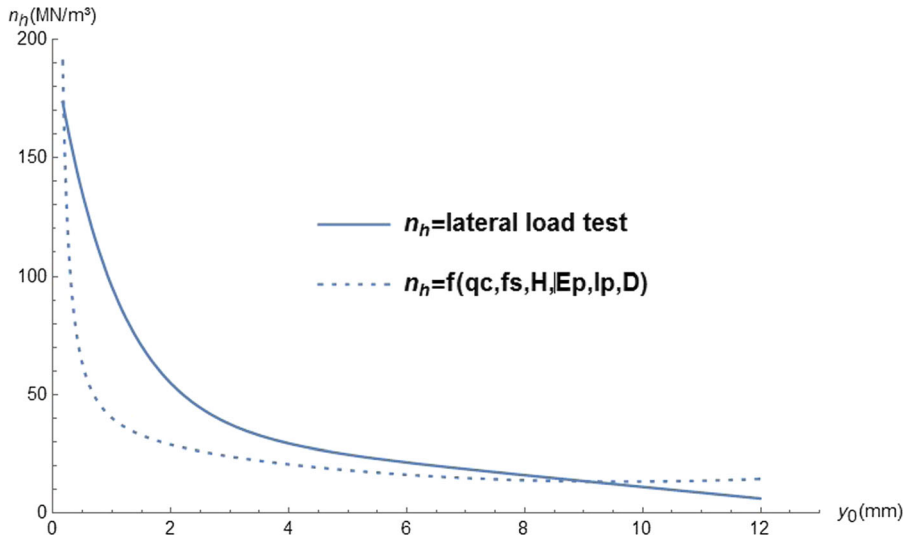

Fig. 17 Comparison between constant horizontal subgrade reaction: lateral load test and Eq. (31)

Table 4 Comparison between methodology, to determine n_h

y_o (mm)	n_h (load test) (MN/m^3)	$n_h(q_c)$ (MN/m^3)	$n_{h(Ave)}$ (load test) (MN/m^3)	$n_{h(Ave)}(q_c)$ (MN/m^3)
4	29.29	20.53	–	–
8	15.98	13.84	20.43	17.18
6	21.34	16.15	–	–
12	6.10	14.38	13.72	15.27

foundation along depth without the use of commercial computer software.

From the values obtained from the the load test on the bored pile ($D = 30$ cm, $L = 5$ m) it were obtained the constant horizontal subgrade reaction soil $n_h = 13.7\,\mathrm{MN/m^2}$ with instrumentation by inclinometers (Fig. 4) and load testing (Fig. 5) in the experimental field at Unicamp, where the results of the inclinometers are compared with the analytical model for some loading stages shown in Figs. 20, 21 and 22. The analytical model had good agreement with the three loading stages, since the pile failure occurred at 49 kN. Then, it has the efficiency of the analytical model for sizing of foundations when having the pile's lateral loading test. Furthermore, this review presents the calibration of the Miche analytical model with data from the inclinometer of the lateral load test. That is, for each set of deflection versus depth values and cutting parameters, the constant horizontal subgrade reaction is determined using the least squares method applied to the Miche displacement analytical solution.

5 Conclusion

The problem of piles with horizontal top loading was solved analytically by Taylor series, wherein generalized hypergeometric functions were the solution. The solution for displacement, moment and shear is compared with the problem numerically solved by Miche (1930). A new equation for the top displacement calculation was found, and displacement was shown to also depend on pile displacement. In the case of the generalized analytical model, a new equation was found to determine the maximum moment and point of application for different forms of the horizontal soil reaction coefficient. The analytical model, unlike Miche's numerical model (1930), is

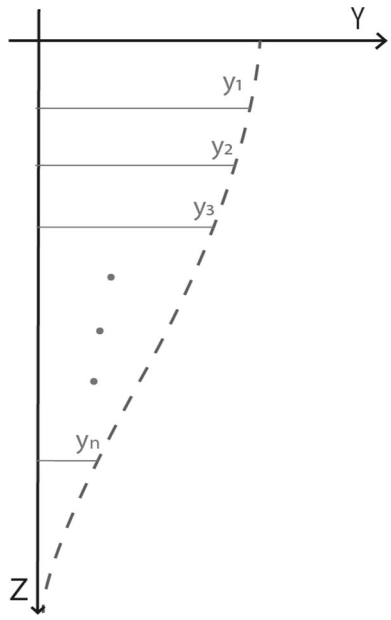

Fig. 18 Displacement according to inclinometer measurement

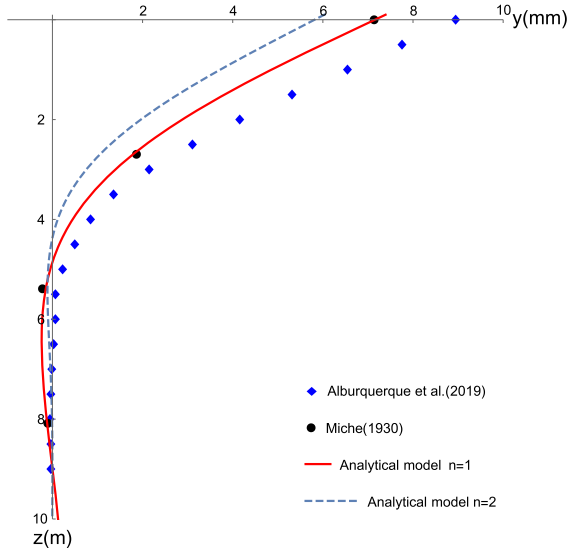

Fig. 19 Comparison between analytical and experimental models

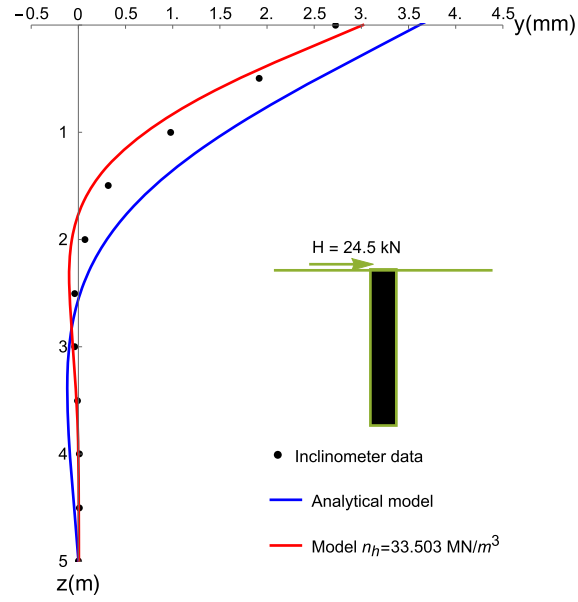

Fig. 20 Comparison between analytical, model and inclinometer data

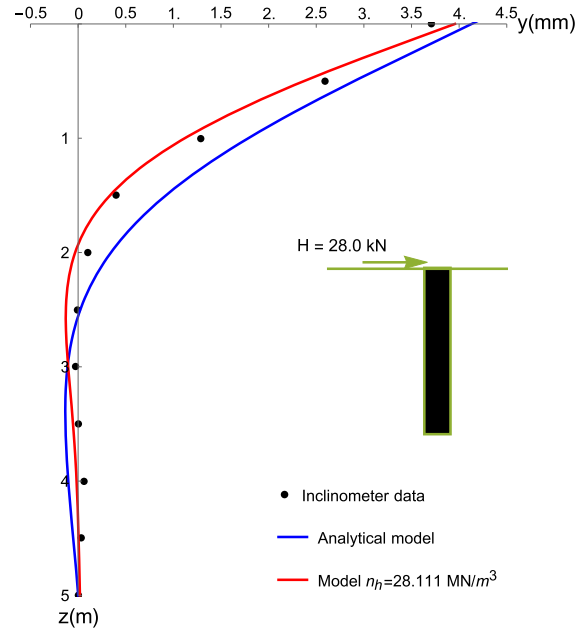

Fig. 21 Comparison between analytical, model and inclinometer data

continuous and can be used for calibration in pile dimension problems, with measurements of field inclinometers when performing lateral loading tests. The analytical model adjusted the inclinometer measurements of an bored pile very well, thus showing good agreement with the experimental data. The proposal for a formulation to obtain the n_h curve based on the data from the CPT test is promising and to be validated it must have other lateral load tests. For future studies, Miche's fractional model should be solved and compared with the experimental data, since

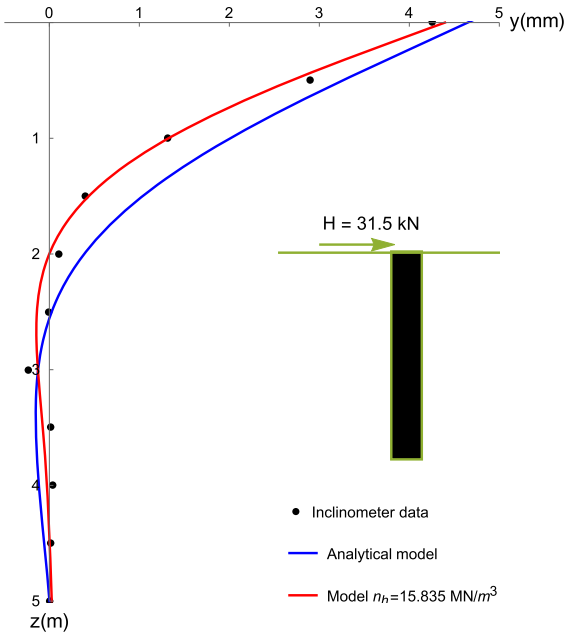

Fig. 22 Comparison between analytical, model and inclinometer data

the analytical solution is given in terms of the Mittag–Leffler functions derived from fractional calculus.

Appendix

By substituting Eq. (6) for Eq. (1), and developing the sum to $n = 4$ in the first part:

$$\sum_{n=4}^{\infty} n(n-1)(n-2)(n-3)a_n z^{n-4} + \beta^5 \sum_{n=0}^{\infty} a_n z^{n+1} = 0 \tag{34}$$

Turning $n \to n+4$ in the first installment of the equation and $n \to n-1$ for the second installment, it has:

$$\sum_{n=0}^{\infty} (n+1)(n+2)(n+3)(n+4)a_{n+4} z^n + \beta^5 \sum_{n=1}^{\infty} a_{n-1} z^n = 0 \tag{35}$$

Rearranging this, we have

$$1 \cdot 2 \cdot 3 \cdot 4a_4 + \sum_{n=1}^{\infty} [(n+1)(n+2)(n+3)(n+4) a_{n+4} + \beta^5 a_{n-1}] z^n \tag{36}$$

So that $a_4 = a_9 = \cdots = a_{5n+4} = 0$, and a_0, a_1, a_2 and a_3 are arbitrary, so the recurrence relationship is provided by

$$a_{n+4} = -\frac{\beta^5 a_{n-1}}{(n+1)(n+2)(n+3)(n+4)}. \tag{37}$$

Considering $n = 1, 2, 3, 4$, in Eq. (37), it has

$$a_5 = \frac{-\beta^5 a_0}{2 \cdot 3 \cdot 4 \cdot 5},$$
$$a_6 = \frac{-\beta^5 a_1}{3 \cdot 4 \cdot 5 \cdot 6},$$
$$a_7 = \frac{-\beta^5 a_2}{4 \cdot 5 \cdot 6 \cdot 7},$$
$$a_8 = \frac{-\beta^5 a_3}{5 \cdot 6 \cdot 7 \cdot 8}.$$

Furthermore, for $n = 6, 7, 8, 9$, in Eq. (37), and using the previous equations:

$$a_{10} = \frac{\beta^{10} a_0}{2 \cdot 3 \cdot 4 \cdot 5 \cdot 7 \cdot 8 \cdot 9 \cdot 10}$$
$$a_{11} = \frac{\beta^{10} a_1}{3 \cdot 4 \cdot 5 \cdot 6 \cdot 8 \cdot 9 \cdot 10 \cdot 11}$$
$$a_{12} = \frac{\beta^{10} a_2}{4 \cdot 5 \cdot 6 \cdot 7 \cdot 9 \cdot 10 \cdot 11 \cdot 12}$$
$$a_{13} = \frac{\beta^{10} a_3}{5 \cdot 6 \cdot 7 \cdot 8 \cdot 10 \cdot 11 \cdot 12 \cdot 13}$$

By applying the same process to infinite values of n, it has the behavior of a generalized hypergeometric function, as defined in Eq. (3). The general solution of Eq. (2) is achieved by substituting the terms a_n found in the Taylor series given by Eq. (3), therefore,

$$
\begin{aligned}
y[z] = a_0 & \left(1 - \frac{(\beta^5 z^5)^1}{2\cdot 3\cdot 4\cdot 5} + \frac{(\beta^5 z^5)^2}{2\cdot 3\cdot 4\cdot 5\cdot 7\cdot 8\cdot 9\cdot 10} \right. \\
& \left. - \frac{(\beta^5 z^5)^3}{2\cdot 3\cdot 4\cdot 5\cdot 7\cdot 8\cdot 9\cdot 10\cdot 12\cdot 13\cdot 14\cdot 15} + \cdots \right) \\
& + a_1 z\beta \left(1 - \frac{(\beta^5 z^5)^1}{3\cdot 4\cdot 5\cdot 6} + \frac{(\beta^5 z^5)^2}{3\cdot 5\cdot 6\cdot 8\cdot 9\cdot 10\cdot 11} \right. \\
& \left. - \frac{(\beta^5 z^5)^3}{3\cdot 4\cdot 5\cdot 6\cdot 8\cdot 9\cdot 10\cdot 11\cdot 13\cdot 14\cdot 15\cdot 16} + \cdots \right) \\
& a_2 z^2\beta^2 \left(1 - \frac{(\beta^5 z^5)^1}{4\cdot 5\cdot 6\cdot 7} + \frac{(\beta^5 z^5)^2}{4\cdot 5\cdot 6\cdot 7\cdot 9\cdot 10\cdot 11\cdot 12} \right. \\
& \left. - \frac{(\beta^5 z^5)^3}{4\cdot 5\cdot 6\cdot 7\cdot 9\cdot 10\cdot 11\cdot 12\cdot 14\cdot 15\cdot 16\cdot 17} + \cdots \right) \\
& a_3 z^3\beta^3 \left(1 - \frac{(\beta^5 z^5)^1}{5\cdot 6\cdot 7\cdot 8} + \frac{(\beta^5 z^5)^2}{5\cdot 6\cdot 7\cdot 8\cdot 10\cdot 11\cdot 12\cdot 13} \right. \\
& \left. - \frac{(\beta^5 z^5)^3}{5\cdot 6\cdot 7\cdot 8\cdot 10\cdot 11\cdot 12\cdot 13\cdot 15\cdot 16\cdot 17\cdot 18} + \cdots \right)
\end{aligned} \tag{38}
$$

References

Ai ZY, Feng DL, Cheng YC (2013) Bem analysis of laterally loaded piles in multi-layered transversely isotropic soils. Eng Anal Bound Elem 37(7–8):1095–1106

Albuquerque PJR, Carvalho Dd, Kassouf R, Fonte NL Jr (2019) Behavior of laterally top-loaded deep foundations in highly porous and collapsible soil. J Mater Civ Eng 31(2):04018373

Alizadeh M, Davisson M (1970) Lateral load tests on piles-arkansas river project. J Soil Mech Found Div

API R (2000) 2a-wsd. Recommended practice for planning, designing and constructing fixed offshore platforms-working stress design 21

Ayyub BM, McCuen RH (2015) Numerical analysis for engineers: methods and applications. Chapman and Hall/CRC, Boca Raton

Banerjee P, Davies T (1978) The behaviour of axially and laterally loaded single piles embedded in nonhomogeneous soils. Geotechnique 28(3):309–326

Basu D, Salgado R, Prezzi M (2009) A continuum-based model for analysis of laterally loaded piles in layered soils. Geotechnique 59(2):127–140

Budhu M, Davies TG (1988) Analysis of laterally loaded piles in soft clays. J Geotech Eng 114(1):21–39

Erdélyi A (1955) Higher transcendental functions. In: Erdelyi A (ed) Higher transcendental functions, vol 1–3. McGraw-Hill, New York, pp 263–267

Froio D, Rizzi E (2017) Analytical solution for the elastic bending of beams lying on a linearly variable winkler support. Int J Mech Sci 128:680–694

Garcia JR (2015) Análise experimental e numérica de radiers estaqueados executados em solo da região de campinas/sp. Universidade Estadual de Campinas, São Paulo, Brazil, Tese de Doutorado

Gon FS (2011) Caracterização geotécnica através de ensaios de laboratórios de um solo de diabásio da região de campinas/sp. Universidade Estadual de Campinas, São Paulo, Brazil, Dissertação de mestrado

Gupta BK, Basu D (2017) Analysis of laterally loaded short and long piles in multilayered heterogeneous elastic soil. Soils Found 57(1):92–110

Hetenyi M (1946) Beams on elastic foundation, University of Michigan studies. Wiley, Hoboken

King AC, Billingham J, Otto SR (2003) Differential equations: linear, nonlinear, ordinary, partial. Cambridge University Press, Cambridge

Liang F, Li Y, Li L, Wang J (2014) Analytical solution for laterally loaded long piles based on Fourier–Laplace integral. Appl Math Model 38(21–22):5198–5216

Matlock H (1970) Correlations for design of laterally loaded piles in soft clay. In: Offshore technology in civil engineering's hall of fame papers from the early years, pp 77–94

Matlock H, Reese LC (1961a) Foundation analysis of offshore pile supported structures. Conf Soil Mech Found Eng 2:91–97

Matlock H, Reese LC (1961b) Foundation analysis of offshore pile supported structures. Conf Soil Mech Found Eng 2:91–97

Miche R (1930) Investigation of piles subject to horizontal forces. Appl Qualy Walls J School Eng (4)

Oliveira ECd, Tygel M (2005) Métodos matemáticos para engenharia. SBMAC, São Carlos

Phanikanth V, Choudhury D, Reddy GR (2010) Response of single pile under lateral loads in cohesionless soils. Electron J Geotech Eng 15(10):813–830

Phanikanth V, Choudhury D, Srinivas K (2013) Response of flexible piles under lateral loads. Indian Geotech J 43(1):76–82

Poulos HG (1971a) Behavior of laterally loaded piles I. Single piles. J Soil Mech Found Div, pp 711–731

Poulos HG (1971b) Behavior of laterally loaded piles pile groups. J Soil Mech Found Div, pp 733–751

Reese L, Nyman K (1978) Field load test of instrumented drilled shafts at Islamorada, Florida. In: A report to girdler foundation and exploration corporation. Clearwater, Florida pp 1–150

Reese LC, Matlock H (1960) Numerical analysis of laterally loaded piles. In: Proceedings, second structural division conference on electronic computation. American Society of Civil Engineers, pp 657–668

Reese LC, Welch RC (1975) Lateral loading of deep foundations in stiff clay. J Geotech Geoenviron Eng 101(ASCE# 11456 Proceeding)

Reese LC, Cox WR, Koop FD (1974) Analysis of laterally loaded piles in sand. In: Offshore technology in civil engineering hall of fame papers from the early years, pp 95–105

Robertson PK (1990) Soil classification using the cone penetration test. Can Geotech J 27(1):151–158

Robertson PK, Cabal K (2015) Guide to cone penetration testing for geotechnical engineering. Gregg Drilling and Testing, Signal Hill

Robin W (2014) On the procedure for the series solution of certain general-order homogeneous linear differential equations via the complex integration method. Nonlinear Anal Differ Equ 2:155–171

Salgado R, Tehrani F, Prezzi M (2014) Analysis of laterally loaded pile groups in multilayered elastic soil. Comput Geotech 62:136–153

Shen W, Teh C (2002) Analysis of laterally loaded pile groups using a variational approach. Geotechnique 52(3):201–208

Sun K (1994) Laterally loaded piles in elastic media. J Geotech Eng 120(8):1324–1344

Van Impe WF, Reese LC (2010) Single piles and pile groups under lateral loading. CRC Press, Boca Raton

Verruijt A, Kooijman A (1989) Laterally loaded piles in a layered elastic medium. Geotechnique 39(1):39–46

Vos J (1982) The practical use of CPT in soil profiling. In: Proceedings, Second european symposium on penetration testing. ESOPT-2, Amsterdam, May 24–27, Vol 2, pp. 933–939

Welch RC, Reese LC (1972) Laterally loaded behavior of drilled shafts. Center for Highway Research University of Texas, Austin, pp 65–89

Zhang L, Ernst H, Einstein HH (2000) Nonlinear analysis of laterally loadedrock-socketed shafts. J Geotech Geoenviron Eng 126(11):955–968